

## Simulations of Two Patterns Fiber Weaves Reinforced in Rubber Actuator

Ili Najaa Aimi Mohd Nordin<sup>a\*</sup>, A. A. M. Faudzi<sup>a,b</sup>, M. R. M. Razif<sup>a</sup>, E. Natarajan<sup>c</sup>, S. Wakimoto<sup>d</sup>, K. Suzumori<sup>d</sup>

<sup>a</sup>Control and Mechatronics Engineering Department, Faculty of Electrical Engineering, Universiti Teknologi Malaysia, 81310 UTM Johor Bahru, Johor, Malaysia

<sup>b</sup>Center for Artificial Intelligence and Robotics (CAIRO), University Teknologi Malaysia, 81310 UTM Johor Bahru, Johor, Malaysia

<sup>c</sup>School of Mechanical Engineering, Kolej Universiti Linton, Mantin, Negeri Sembilan, Malaysia

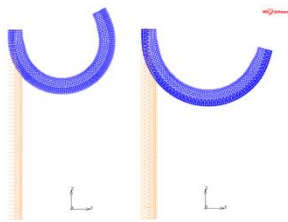
<sup>d</sup>Graduate School of Natural Science and Technology, Okayama University, 3-1-1, Tsushima-naka, Kita-ku, Okayama, 700-8530, Japan

\*Corresponding author: athif@fke.utm.my

### Article history

Received :12 April 2014  
Received in revised form :  
7 June 2014  
Accepted :2 July 2014

### Graphical abstract



### Abstract

Over recent years, studies on soft mechanism are rapidly being paid to attention especially in pneumatic actuator field. A good actuator should be able to provide sufficient force and flexibility in movement, hence bending motion is a vital criteria needed in soft robotic actuation. In this paper, a solution to soft bending pneumatic actuator is proposed in which several patterns fiber weave designs are introduced. The objectives of the simulations is to investigate the different weave patterns combination of fiber reinforced actuator models that yields the best bending characteristics and its relation to the contraction or extension characteristics shown by single weave pattern actuator models. From the results, when two patterns of fiber weave were attached together to form a sleeve, significant bending were obtained from most of the models simulated. Large bending resulted from combined two patterns fiber weave models were achieved when maximum contraction and extension characteristics exhibited by both fiber weave patterns.

**Keywords:** Soft actuator; pneumatic artificial muscles; McKibben actuator

© 2014 Penerbit UTM Press. All rights reserved.

### › 1.0 INTRODUCTION

Soft actuators have been vigorously utilized in many applications in modern society these days. Soft actuation mechanism driven by these type of actuators are very useful in various robotics and automation applications, for example; in object transportation, bio-mimetic, endoscopy insertion, micro manipulation of handling micro scale object, robotic gripper, power support and assisting rehabilitation exercises. The existing developed soft actuators have shown promises in producing soft movements to objects and human [1-22].

A soft actuator generally has simple structure, high compliance, high power to weight ratio, high water resistance, lightweight and requires low production cost [2, 3, 6-8, 11]. It is usually being made from soft materials such as rubber and silicone. The actuator functions due to elastic deformations of extension and contraction of the elastic structure from silicone or rubber when air is pressurized into it [2-3, 11-12].

Knowing the capability of pneumatic soft actuator in producing soft movement, improvement in achieving better bending and actuating force suitable to applications still need to be done, thus has attracted many researchers to dig deeper into this area. There are many existing methods to exhibit good bending and force characteristics. The approaches towards designing bending actuator have been mainly based on chambers-type [3, 8], bellow shape-type [4, 6, 7, 22] and fiber-reinforced-type [2, 5, 22].

Bending soft actuator that works based on the principle of the two internal chambers was achieved by Suzumori, Endo *et al.* [3]. The bending movement was utilized for a robot that mimics the manta features to repeatedly flap in two directions. The robot was tested and it can lively swim in the water.

Bellow shape-type actuator invented by K. Ogura *et al.* was able to produce large curling motion deformation in two directions. The actuator can facilitate the curling motion as a miniature robot hand for handling fragile fish eggs [6-7].

Another bending technique which uses fiber reinforced weaving was able to create bending motion for application that requires high force [12]. The actuator works by pressurizing both contracted and extended type actuators which these actuators are bound together.

Besides being used as a biomimetic robot [3] and gripper [6-7], soft actuator designs are also used in medical application. The actuator was developed using silicone rubber material and aimed to help doctors in performing colonoscopy insertion. The prototype of the large intestine endoscope has shown capability of changing its own stiffness, which has made colonoscopy insertion procedure to be much faster and accurate. It is able to avoid overload for inner colon overload and realize safety check. The actuator incorporates fiber-reinforced weaving technique inspired by McKibben artificial muscle to produce this stiffness-change device [5].

The last two soft actuator designs incorporates the fiber reinforced weaving technique inspired by McKibben artificial

muscle to produce bending [12] and stiffness-change [5]. The McKibben artificial muscle was first invented by Joseph L. McKibben and used as an orthotic appliance for polio patients. It is well known to be light in weight, able to produce smooth, accurate and fast response even significant force at its maximum expansion [13].

In recent years, the effects of braided fiber angles to soft actuator contraction and extension motion were studied [5,12,17,20]. Generally, the McKibben actuator will contract axially when air pressure is inserted. Contraction ratio can be obtained from the force equation from Schulte model [17] described in Equation (1), as below:

$$\dots - \dots \quad (1)$$

Where;

- F = contraction Force,
- $d_0$  = actual diameter of the actuator in initial state,
- $p$  = applied pressure,
- $\alpha_0$  = initial fiber angles and
- $\lambda$  = contraction ratio.

In this equation, the length of actuator is assumed to be infinity and the fiber is able to resist stretching. The friction between rubber tube and braided fibers, and the elasticity of the rubber tube will not affect the force generated.

The McKibben-type artificial muscle actuator begins to contract when compressed air is provided to the actuator [17]. The contraction force is decreasing as contraction increases. The contraction ratio, [5, 17] when the contraction force is 0N, is described in the following equation:

$$\dots \propto \dots \quad (2)$$

Calculation based on Equation (2) shows that fiber angles of  $0^\circ$  to  $76.6^\circ$  result in positive contraction ratio depicting existence of contraction in length. Whereas fiber angles  $90^\circ$  to  $54.7^\circ$  will result in negative contraction ratio which describe extension in length. When the fiber angle is  $54.7^\circ$ , the contraction ratio is 0 which shows that there is no contraction or extension in length. Figure 1 shows the initial and after conditions of the artificial muscles actuator after being pressurized with 1.5MPa of air. In Figure 1, the actuators were fabricated with fiber weave of  $66.5^\circ$ ,  $54.7^\circ$   $23.5^\circ$  respectively (top to bottom). Figure 1(a) shows the actuators condition before pressure was applied. The after conditions of the first actuator, as in Figure 1 (b) shows an increment in length while the third actuator shows decrement in length resulting from contraction motion of its body. However, the second actuator does not show any changes in length but stiffness change was realized. The results proved that the contraction and extension of a single chamber actuator with single weave fiber angle reinforcement depends on the fiber weave angles.

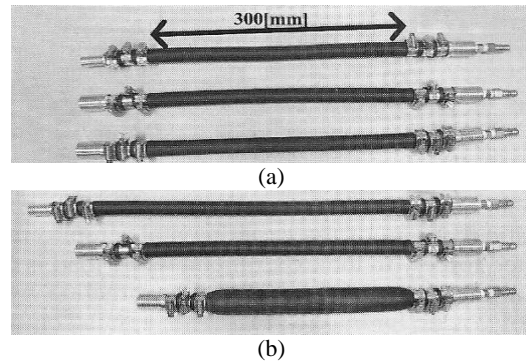


**Figure 1** Three types of Pneumatic Artificial Muscles (Extending, Stiffness-change and Contracting-type), (a) before applying pressure (b) after applying pressure [12]

The objective of the paper is to investigate different weave patterns combination of fiber reinforced actuator models that yields the best bending characteristics and its relation to the contraction/extension characteristics shown by single weave pattern actuator models. Various fibers angles and patterns were tested and the displacement results from the actuator models were compared.

The analyses were carried out as static analysis using numerical solutions from the Finite Element MARC Mentat software. Until present, there are several studies that use MARC deformation cases. Most of them proved good agreement between experimental and simulation results [2, 3,5-7].

**> 2.0 DESIGN CONCEPT**

Study done by [12] has proved that fiber weave angle of  $23.5^\circ$  will lead to contraction and  $66.5^\circ$  will result in extension of the actuator length and the attachment of both actuators; contracted and extended soft actuators will bend the whole body to the contracted actuator side. Hence, it is expected that by attaching two different weave angles reinforced to a single chamber soft actuator will also produce bending motion.

A single chamber with two patterns fiber weave on each half of its cylindrical tube connected at both ends to fittings is proposed and is illustrated in Figure 2. The method of combining two different angles of fiber reinforced around a single chamber soft actuator has been experimentally proven in [15] that the design can produce bending motion.

The bending actuator design was inspired from the principles of contraction and extension of artificial muscle. In Figure 3, fiber weave angle  $\alpha_1$  represents the angle at half one side of the actuator, predicted to produce contraction motion while  $\alpha_2$  at the other half side of the body is anticipated for extension motion. With contraction and extension motion acting on single chamber actuator, the body should bend to the contracted side.

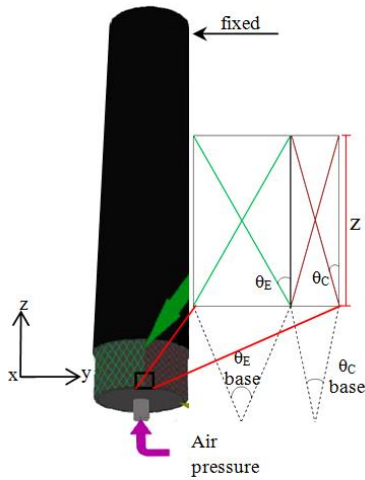


Figure 2 Bending soft actuator braided by two patterns fiber weaves.

3.0 SIMULATION MODEL

In this paper, the actuators were modeled as three layers cylindrical structure, same with actuators in [14, 15]. However, different rubber and fiber materials were used. In this case, silicone rubber KE1603 A-B rubber and Nylon fiber were selected due to the realibility of Mooney-rivlin property for silicone rubber and linear property for Nylon fiber [2, 3, 5-7]. As shown in Figure 3; the first inner layer is modeled as silicone rubber, second is weave layer from Nylon and outer is from the same type silicone rubber. The thickness of inner rubber layer is 2 mm and outer layer is 1 mm. The total length of actuator is 170 mm including caps fittings at both end with each of them 10 mm length.

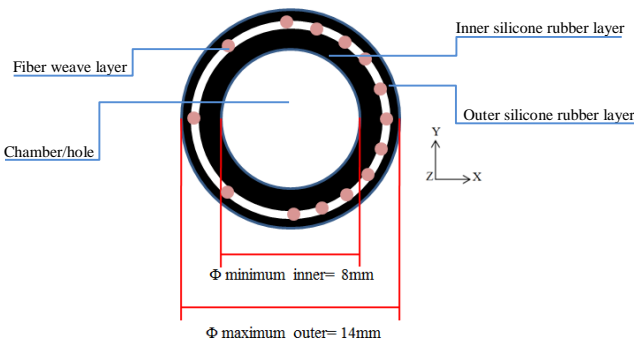


Figure 3 2-D views of the base actuator model

Bending actuators presented in this paper are different from the studies in [14,15]. Actuator in [15] has similar dimension like actuator proposed in this paper but the fiber angles 84° and 79° cannot be modeled due to modeling technique restriction. Plus, different materials were used in [14] and [15] which is natural rubber weaved by aramid fiber, and Silastic P1 rubber weaved by cotton fiber respectively.

Study on the characteristics of actuators modeled from single weave pattern reinforced to the actuator body was conducted. Eight models from different fiber weave conditions were investigated for any resulting motions. Figure 4 shows the weave pattern designs that being varied. The 32-deg (Model 1) and 43-deg (Model 2) fiber angle models are predicted to produce contraction in length, 62-deg (Model 3) and 70-deg (Model 4) fiber angles to produce extension in length, 90-deg (Model 5) anticipated also for extension while 0-deg (Model 6) for contraction. Plain Weave, PW design (Model 7)

is fibers attachment of 0° and 90° braided together not known for any motion also considered for simulation. Actuator with no fiber attachment (Model 8) was also simulated to realize the impact of fibers reinforcement to the actuator. The hypotheses are made based on theoretical calculations from Equation (2).

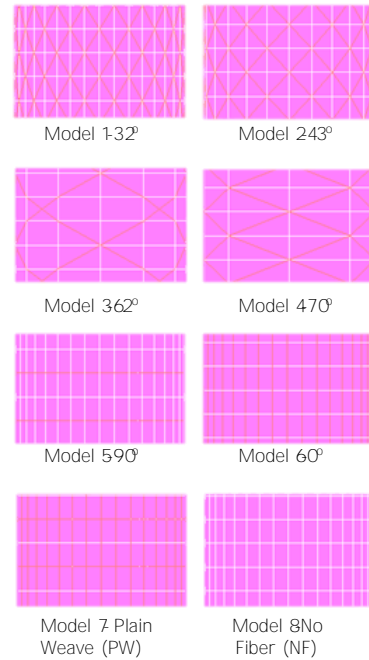


Figure 4 2-D views of single pattern fiber weave. Orange lines represent the fibers

The combined two patterns fibers weave design specifications for bending motion analysis is shown in Table 1. Ten models were investigated for bending motion.

Table 1 Two weave fiber pattern characteristics

Model	Fiber pattern at left side	Fiber pattern at right side
1	70-degree	32-degree
2	62-degree	32-degree
3	70-degree	43-degree
4	62-degree	43-degree
5	90-degree	32-degree
6	70-degree	90-degree
7	0-degree	32-degree
8	70-degree	0-degree
9	No Fiber, NF	32-degree
10	70-degree	No Fiber, NF

Table 2 Properties of Finite Element Method (FEM) analysis

Properties	Cylindrical-like Rubber layers	Fiber
Element type	Quadratic (4 element nodes)	Line (2 element nodes)
Geometrical properties	3-D solid	3-D truss
Material properties	Silicone rubber KE1603 A-B; ShinEtsu Silicones Third order Mooney-rivlin function $C_{10}= 0.0863497$ $C_{01}= 0.0621348$ $C_{11}= -0.0128964$ $C_{20}= 0.00342553$ $C_{30}= -0.657745$	Nylon Linear-elastic function $[ q w p i \phi u " O q f w n w u " ?$ $R q k u u q p \phi u " T c v k q$
Contact properties		Deformable Glued to each other
Analysis method		Static structural analysis with Full Newton-Raphson iterative procedure
Analysis option		Large deformation analysis

4.0 SIMULATION SETUP

MARC Mentat software is one of the powerful solvers to nonlinear analysis problem. The software is used to carry out simulation problems under static, dynamics or multi-physics loading assumptions. In this study, all models were configured to have same build-in parameter setup. Note that all models differ in fiber weave pattern embedded to its inner rubber layer. Table 2 shows the properties setting of Finite Element Method (FEM) analysis conducted.

Two boundary conditions were applied. The nodes at one end of the actuator were fixed at X, Y and Z directions and pressure of 205 OR c " y c u " c r r n k g f " v q " v j g " k p p as illustrates in Figure 5.

Before actuator models of two patterns fiber weave were simulated, actuator models of single pattern fiber weave reinforced to its cylindrical inner rubber layer tube were studied. This is to characterize the properties of each pattern fiber weave whether they exhibits contraction, extension, twisting or other motions.

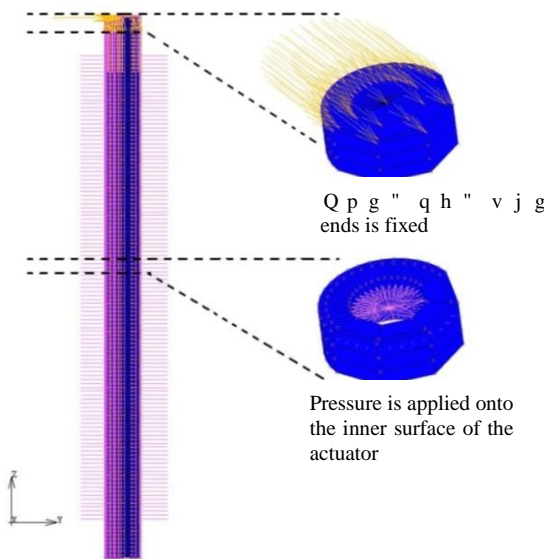


Figure 5 Boundary conditions

5.0 RESULTS AND DISCUSSION

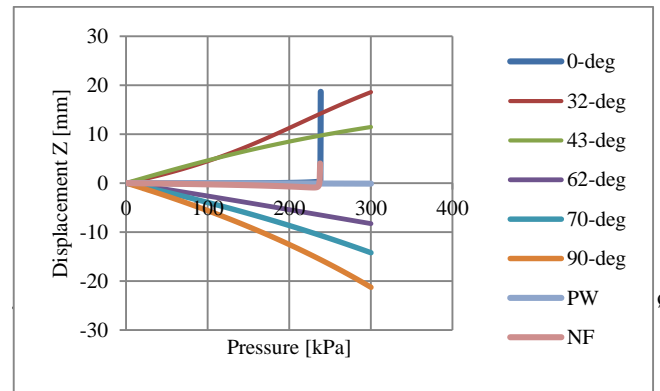


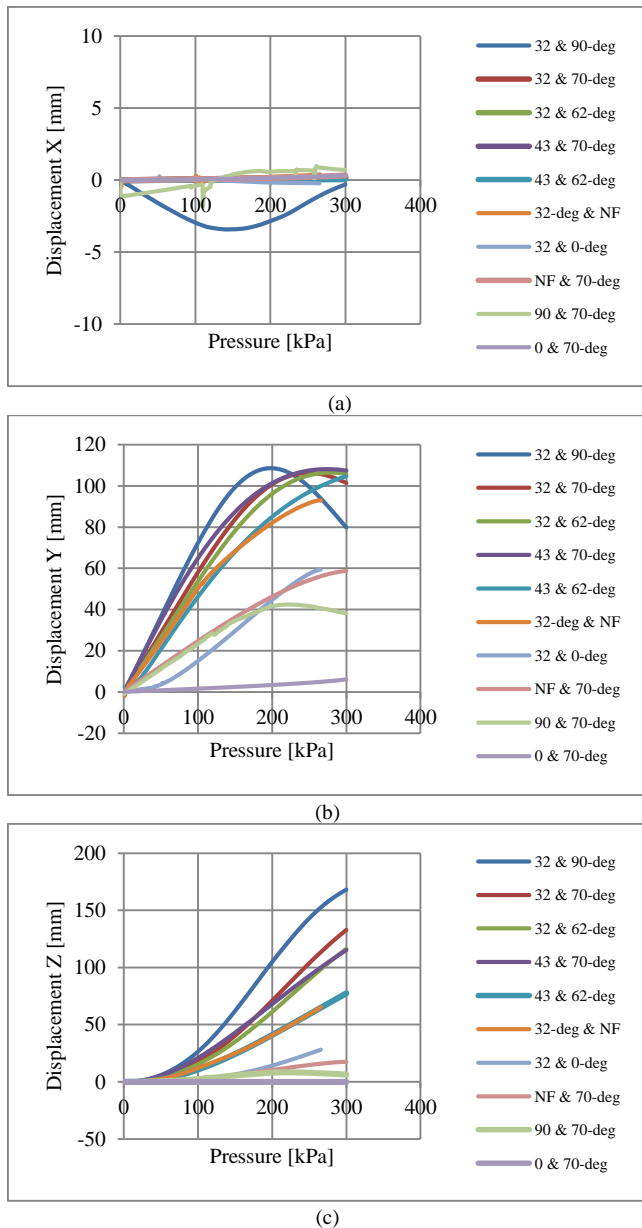
Figure 6 Displacement at Z axis of single weave pattern actuator

Figure 6 presents the displacement at Z-axis of several single pattern fibers weave embedded to the inner layer of the actuator. As predicted from theoretical equation, the fibers angle 32°, 43° and 0° shows positive displacement in simulations, which signify contraction in length, agreed to the theoretical calculation, but 0° model does not contract before 238.5 kPa. 62°, 70° and 90° models show negative displacement expressing extension in length at Z direction, also agreed with theoretical outputs.

Table 3 Single pattern weave actuator models characterization

Weave type	Fiber angle [degree]	Contraction ratio from Eq. 2	Characteristic shown from Eq. 2	Characteristic shown from simulation
Braid	32	0.32	contraction	contraction
	43	0.21	contraction	contraction
	62	-0.23	extension	extension
	70	-0.69	extension	extension
Single	; 2 é :	-330796.33	extension	extension
Single	0	0.42	contraction	Sudden contraction at 238.5 kPa
Plain	-	-	-	No deformation
No Fiber	-	-	-	Sudden contraction at 238 kPa

The Plain weave-type does not show any major expansion, extension and contraction in length and mostly remain static even the pressure increases. Therefore, Plain Weave pattern will not be considered for two patterns fiber weave actuator analysis. For No Fiber model (NF), small sudden contraction is observed at 238 kPa but no significant changes in length measured before that. This proved that fiber reinforcement to rubber actuator could improve bending motion. All fiber patterns were considered for two patterns fiber weave analysis except Plain weave (PW) fiber pattern. Easy comparisons are shown in Table 3.



**Figure 7** Results of nonlinear FEM of several models of combined two weave patterns actuator: (a) Displacement at X direction, (b) Y direction and (c) Z direction

Figure 7 (a) shows the results of nonlinear FEM, where horizontal axis is the air pressure and the vertical axis defined as displacement. From the graph, most of the models show almost 0 displacements except Model 32° and Model 70° that combined with 90°.

From Figure 7(b) and (c), the model that shows maximum displacement in Y and Z axis is the 32° with 90° fiber angles combination, followed by 32° & 70°, 32° & 62°, 43° & 70°, 43° & 62°, 32° & NF, 32° & 0°, NF & 70°, 90° & 70° and lastly 0° & 70°. The bending motions of the best two models are presented in Figure 9.

Actuators with combined patterns of extension and contraction show bending motion, but a combined pattern of same characteristic from both left and right weave will reduce their bending capability. This can be observed from Model 32° & 0° and 90° & 70° where the displacement of Model 32° & 0° is lesser than 32° with no fibers combination and Model 90° & 70° is lesser than 70° degree with no fibers combination.

In addition, any combinations with 0° pattern do not show good displacement, even single pattern analysis of 0° also shows no contraction before 238.5kPa; referring to Figure 6.

All models present similar curling motion, as shown in Figure 8. Several models that show high bending motion will be considered for further comparison with fabricated model in the future. Figure 9 shows bending displacements of the best two models, Model 32° & 90° and Model 32° & 70°.

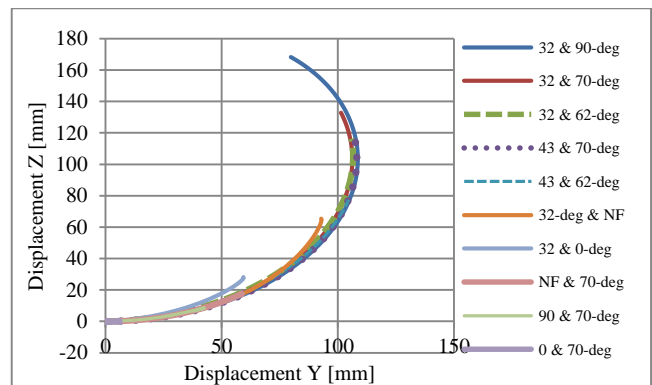


**Figure 8** Trajectories of the actuator tip of two patterns fiber weave actuator from analytical results

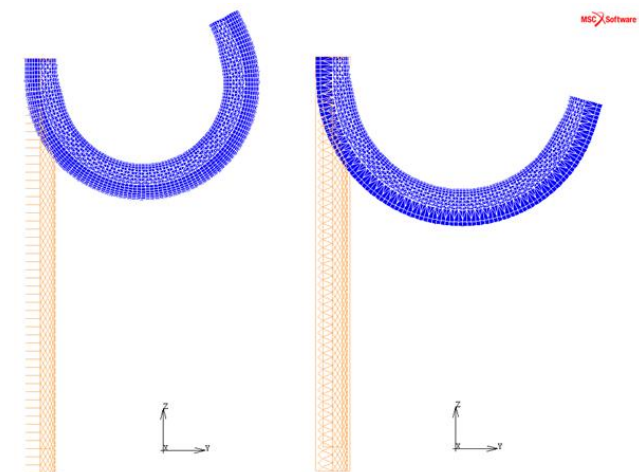


**Figure 9** Bending displacements of the best two models; Model 32° & 90° (left) and Model 32° & 70° (right). Orange lines represent initial position of the actuator and blue is the final position of the actuator after 300 kPa pressure was applied

## 6.0 CONCLUSION

A solution to bending actuator is proposed in which several patterns fiber weave designs were introduced. The bending motions generated from actuators were presented through deformation of c e v w c v q t ø u-axis directions with increase in pressure. When two patterns of fiber weave are attached together to form a sleeve, significant bending were obtained from most of the models simulated.

Large bending resulted from combined two patterns fiber weave models is achieved when maximum contraction and extension characteristics are exhibited from the model. Combinations of weave patterns of fiber reinforced actuator models that yield the best bending characteristics and its relation to the contraction or extension characteristics have been identified. From the results, 32° weave pattern shows the highest contraction while 90° shows the highest extension, both in Z direction. In this study, good bending deformations are obtained from actuators Model 32° & 90° followed by Model 32° & 70° and Model 32° & 62°.

### Acknowledgement

The authors would like to thank Universiti Teknologi Malaysia (UTM) and Ministry of Higher Education (MOHE) Malaysia under ERGS Grant No.Q.J130000.2523.04H90.

### References

- [1] Sasaki, D., T. Noritsugu, et al. 2005. Development of Active Support Splint driven by Pneumatic Soft Actuator (ASSIST). *Proceedings of the IEEE International Conference on Robotics and Automation, ICRA*. 520-525.
- [2] Suzumori, K., T. Hama, et al. 2006. New Pneumatic Rubber Actuators to assist Colonoscope Insertion. *Proceedings IEEE International Conference on Robotics and Automation, ICRA*. 1824-1829.
- [3] Suzumori, K., S. Endo, T. Kanda, N. Kato, and H. Suzuki. 2007. A Bending Pneumatic Rubber Actuator Realizing Soft-bodied Manta Swimming Robot. *IEEE International Conference on Robotics and Automation*. 4975-4980.
- [4] Noritsugu, T., M. Takaiwa, et al. 2008. Power Assist Wear Driven with Pneumatic Rubber Artificial Muscles. *International Conference on Mechatronics and Machine Vision in Practice*.
- [5] Wakimoto, S., I. Kumagai, et al. 2009. Development of Large Intestine Endoscope Changing its Stiffness. *IEEE International Conference on Robotics and Biomimetics, ROBIO*. 2320-2325.
- [6] Wakimoto, S., K. Ogura, K. Suzumori, and Y. Nishioka. 2009. Miniature Soft Hand with Curling Rubber Pneumatic Actuators. *IEEE International Conference on Robotics and Automation, ICRA*. 556-561.
- [7] Ogura, K., S. Wakimoto, K. Suzumori, and Y. Nishioka. 2008. Micro Pneumatic Curling Actuator-Nematode Actuator-. *IEEE International Conference on Robotics and Biomimetics, ROBIO*. 462-467.
- [8] Udupa, G., P. Sreedharan, et al. 2010. Robotic Gripper Driven by Flexible Microactuator based on an Innovative Technique. *IEEE Workshop on Advanced Robotics and Its Social Impacts, ARSO*. 111-116.
- [9] Robert Shepherd F., F. Ilievski, et al. 2011. Multigait Soft Robot. *Proceedings of the National Academy of Sciences of the United States of America*.
- [10] Wang, Y., Z. Wang, et al. 2011. Initial Design of a Biomimetic Cuttlefish Robot Actuated by SMA Wires. *International Conference on Measuring Technology and Mechatronics Automation*.
- [11] Suzumori, K., T. Maeda, et al. 1997. Fiberless Flexible Microactuator designed by Finite-element Model. *IEEE/ASME Transactions on Mechatronics*. 2(4): 281-286.
- [12] Iwata, K., K. Suzumori, et al. 2011. Development of Contraction and Extension Artificial Muscles with Different Braid Angles and their Application to Stiffness Changeable Bending Rubber Mechanism by Their Combination. *Journal of Robotics and Mechatronics*.
- [13] Andrikopoulos, G., G. Nikolakopoulos, and S. Manesis. 2011. A survey on Applications of Pneumatic Artificial Muscles. *IEEE Mediterranean Conference on Control and Automation*. 1439-1446.
- [14] Nordin, I.N.A.M., et al. 2013. 3-D Finite-Element Analysis of Fiber-reinforced Soft Bending Actuator for Finger Flexion. *IEEE/ASME International Conference on Advanced Intelligent Mechatronics*.
- [15] Faudzi, A.A.M., et al. 2012. Development of Bending Soft Actuator with Different Braid Angles. *IEEE/ASME International Conference on Advanced Intelligent Mechatronics*. 1093-1098.
- [16] Ogura, K., S. Wakimoto, K. Suzumori and Y. Nishioka. 2006. Caterpillar Locomotion: A New Model for Soft-bodied Climbing and Burrowing Robots. *International Symposium on Technology and the Mine Problem*.
- [17] Nagase, J. Y., S. Wakimoto, T. Satoh, N. Saga, and K. Suzumori. 2011. Design of a Variable-stiffness Robotic Hand using Pneumatic Soft Rubber Actuators. *Smart Materials and Structures*. 20(10): 105015.
- [18] Daerden, F., and D. Lefeber. 2002. Pneumatic Artificial Muscles: Actuators for Robotics and Automation. *European Journal of Mechanical and Environmental Engineering*. 47(1): 11-21.
- [19] Zhao, F., S. Dohta, and T. Akagi. 2012. Development and Analysis of Bending Actuator Using McKibben Artificial Muscle. *Journal of System Design and Dynamics*. 6(2): 158-169.
- [20] Davis, S., and D. G. Caldwell. 2006. Braid Effects on Contractile Range and Friction Modeling in Pneumatic Muscle Actuators. *The International Journal of Robotics Research*. 25(4): 359-369.
- [21] Noritsugu, T. 2005. Pneumatic Soft Actuator for Human Assist Technology. *JFPS International Symposium on Fluid Power*. 11-20.
- [22] Ilievski, F., D. Aaron, et al. 2011. Soft Robotics for Chemists. *Journal of the Gesellschaft Deutscher Chemiker Angewandte Chemie International Edition*. 50(8): 1890-1895.